Improved Control for Three Phase dual-Stage Grid-Connected PV Systems Based on Predictive Control Strategy

Laib Abdelbaset*, Krim Fateh*, Talbi Billel*, Kihal Abbas*, Feroura Hamza*

** LEPCI Laboratory, Electronics Dept, Setif-1- University Route Bejaia, Setif, Algeria (Tel: +213777159128; e-mail: laib_abdelbaset@univ-setif.dz).*

Abstract: This paper focuses on the control of three phase dual-stage grid connected photovoltaic (PV) system. The control objective is to extract the maximum power delivered by PV array under irradiation variations and to inject it into the network, as well as, the reactive power requested by grid operator while providing high grid currents quality. A fast and accurate control method based on variable step size incremental conductance and predictive current control is proposed and applied to the first stage (DC-DC Boost converter) in order to achieve a fast maximum power point tracking MPPT with less oscillations. Furthermore, a voltage oriented control based on both predictive control strategy and space vector modulation SVM (PS-VOC) is applied to the second stage (Two-level inverter) in order to control the d-q axis grid currents. The proposed system is simulated using Matlab/Simulink and simpower system packages. As results, the proposed MPPT provides a fast and accurate tracking with significant oscillation reduction around the MPP in comparison with conventional methods under irradiation changes. Besides, the injection of the extracted PV power and reactive power requested by the grid operator is provided with high current quality due to the capability of the proposed PS-VOC control method.

Keywords: predictive control strategy, dual-stage grid-connected, maximum power point tracking (MPPT), d-q axis grid current control, solar energy.

1. INTRODUCTION

During the last years, solar energy has attracted a substantial attention to overcome the increased energy consumption and environmental problems (pollution, global warming …etc) (Rong-Jong et al., 2008). Grid connected photovoltaic (PV) systems have been used to inject the energy delivered by the PV arrays into the public grid (Antoneta Iuliana Bratcuet al., 2008 ; Mahrous El-Sayed Ahmed et al. , 2013; Fernando M. de Oliveira et al. , 2016; Abdelkrim Menadi et al. , 2015). The current challenge is to extract the maximum power from the PV arrays and to deliver it to the network with high grid current quality under climatic changes. For this reason, many researchers works on these challenges for two grid PV system topologies namely single and dual stage (Mahrous El-Sayed Ahmed et al. , 2013; Lin Chen et al. , 2014). The latter topology is frequently used due to the fact that MPPT and control of the power injected into the grid are decoupled with different converters. This advantage eases the MPP tracking as well as it boost the DC-link voltage value above the grid peak voltage value despite the produced power (Mahrous El-Sayed Ahmed et al. , 2013).

PV arrays still do not provide a maximum efficiency, since their performance depends on climatic conditions. The random variation of these factors reduces the PV array output power. For this reason, many MPPT techniques have been proposed in the literature in order to force the PV systems to continuously pursuing and rapidly extracting the maximum power from PV generator supply. Conventional MPPT algorithms such as perturb and observe (P&O) (M. Azzouzi, 2013) or Incremental conductance (IncCon) (Azadeh Safari et al., 2011) have been intensively investigated in the last decade (Boualem Bendib et al. ,2015). Nevertheless, these techniques present three major drawbacks: loss of tracking direction, low tracking speed and large oscillations. Recently, several intelligence techniques such as fuzzy logic (Muhammad Ammirrul et al. , 2013 ; Tawfik Radjai et al. , 2014; Mohamed M. Algazar et al. ,2012) and neural networks (Houria Boumaaraf et al. 2015) genetic algorithm (Abdelghani Harrag et al., 2015), particle swarm optimisation (Fernando M. de Oliveira et al. , 2016), have been introduced in order to enhance the performance. However, it is stills difficult to implement them in practically. In addition, Due to the implementation simplicity of the conventional MPPT algorithms, other control schemes based on these algorithms have been proposed to improve the efficiency of PV array by including an internal voltage loop as in MPPT voltage oriented loop (Raseswari Pradhan et al., 2016 ; (Panagiotis E. Kakosimos et al. , 2013) or an internal current loop as in MPPT current oriented loop (Enrico Bianconi et al, 2013 ; Panagiotis E. Kakosimos et al. , 2013). These latter afford an accurate MPP tracking as well as a satisfactory oscillation reduction around the MPP, owing to the linear relation between the PV array current and solar irradiation. Different current controllers are employed in MPPT current oriented loop methods such as PI controller (Sathish Kumar Kollimalla et al. 2014), predictive controller (Panagiotis E. Kakosimos et al., 2013), Finite set predictive controller (Panagiotis E. Kakosimos et al. , 2011) and sliding mode controller (Enrico Bianconi et al, 2013) .Predictive current controller offers significant advantages such implementation simplicity and high performances regarding response time and PV current ripple compared to PI controller.

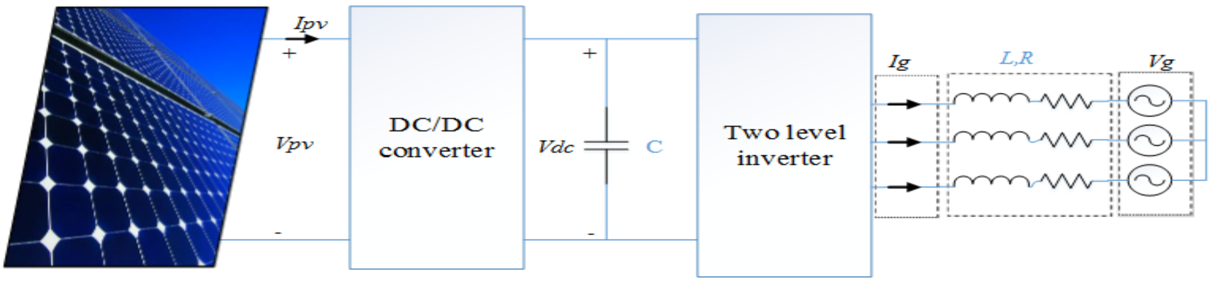

Fig. 1. System Global Configuration

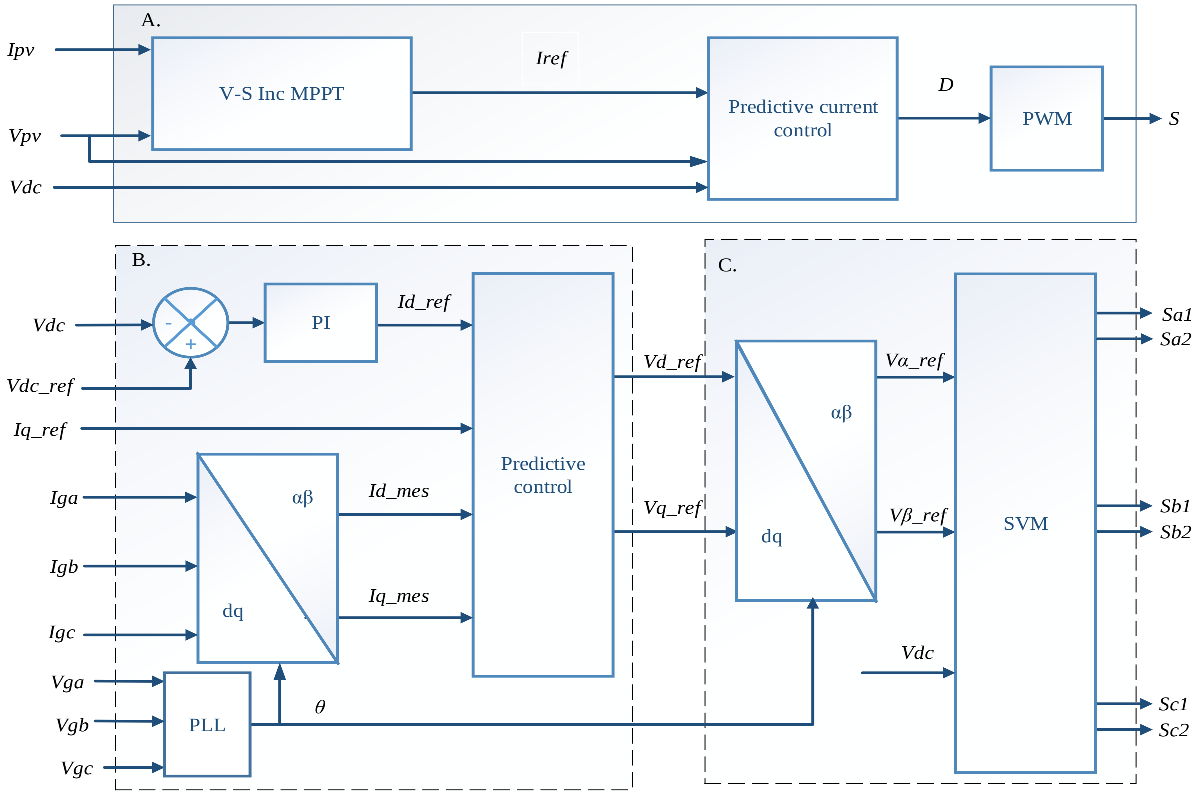

Fig.2.System Global Control

Besides, it has fixed frequency compared to sliding mode and finite set predictive controllers.

In order to obtain better performance in terms of MPP tracking accuracy, dynamic response and oscillation reduction around the MPP. A variable incremental current step size in a MPPT current oriented loop based on predictive current control is proposes as first part this paper.

The second stage is used to inject the extracted PV power into the network with a high gird current quality. For this purpose, many control techniques are proposed. Among them, control methods without modulation stage such as: grid current control based on hysteresis controllers (Chinmay Jain et al. , 2017) or finite set model predictive control strategies (José Rodríguez et al. , 2007), direct power control DPC based on switching table (Jiabing Hu et al., 2011). These techniques provide a high performance. However, they have a variable switching frequency which is a major inconvenient. In the other hand, control method with modulation stage such as: voltage-oriented control (VOC) (Teodorescu Remus et al., 2011), Voltage-based direct power control (V-DPC) (Mariusz Malinowski et al., 2004), Virtual flux oriented control (VFOC) (Mariusz Malinowski et al., 2001) employ PI regulators in internal current control loop in addition to modulation stage (PWM or SVM). It operates with a fixed switching frequency however the slow regulation of PI regulators and control delay deteriorates the performance results.

As second part of this paper, a predictive control strategy is introduced to voltage-oriented control (VOC) based on synchronous frame (d-q) in order to eliminate the control delay and PI regulators drawbacks under PV power injection to the grid with a high grid current quality.

The proposed global system is simulated using Matlab/simulink and simpower system packages, where different tests are carried out in order to check the system performance. Similarly, a comparison in terms of oscillations, accurate tracking and response time is performed between the proposed and conventional MPPT methods. Meanwhile, the Id-Iq currents control and the grid current quality are observed and evaluated under irradiation and reactive power reference change. More details are addressed in subsequent sections.

2. GLOBAL SYSTEM CONFIGURATION

The global system mainly consists of: PV array, DC/DC converter (boost), two level inverter, and R_g, L_g filter tied to grid, as shown in Figure 1.

The PV array generates the power depending on solar radiations. The boost converter is used to track the MPP and to deliver it continuously to the dc link. The two-level inverter injects the power coming from the boost to the grid tacking into account high grid current quality.

3. GLOBAL SYSTEM CONTROL

As shown in Figure 2, the global system is controlled with a three steps technique;

- A Variable step size Incremental conductance through predictive current control strategy is applied to track the MPP rapidly and accurately (VS-IncCon/PCC),
- DC link voltage is regulated by simple PI controller.
- The grid currents are controlled by predictive control strategy through SVM (PS-VOC).

3.1 Improved MPPT control

Under irradiation changes conditions, the current Impp must be tracked rapidly with less ripple to reach the maximum power Pmpp. In this work, MPPT method based on the combination of the conventional current incremental algorithm (Panagiotis E. Kakosimos et al. , 2011) and variable step size algorithm (Fangrui Liu et al., 2008; Abdelhamid Loukriz et al., 2016) is proposed.

A. Variable Current Step Size Incremental Algorithm

The current incremental algorithm as the conventional method is based on the slope of the PV power curve (Azadeh Safari et al., 2011). It identifies the instantaneous position value to the maximum power point; zero at the MPP, positive on the left-hand side of the MPP and negative on the right-hand side of the MPP; *ΔIref* increases when the slope is positive and decreases when it is negative.

The basic equations of this method are as follows:

$$\frac{dP_{pv}}{dI_{pv}} = 0 \qquad (1)$$

Eq (1) can be expressed as:

$$\frac{dp_{pv}}{dI_{pv}} = \frac{d(V_{pv} * I_{pv})}{dI_{pv}} = \frac{dV_{pv}}{dI_{pv}} I_{pv} + V_{pv} \qquad (2)$$

$$\frac{dV_{pv}}{dI_{pv}} I_{pv} + V_{pv} > 0 \quad \text{at left of the MPP} \qquad (3)$$

$$\frac{dV_{pv}}{dI_{pv}} I_{pv} + V_{pv} < 0 \quad \text{at right of the MPP} \qquad (4)$$

$$\frac{dV_{pv}}{dI_{pv}} I_{pv} + V_{pv} = 0 \quad \text{at the MPP} \qquad (5)$$

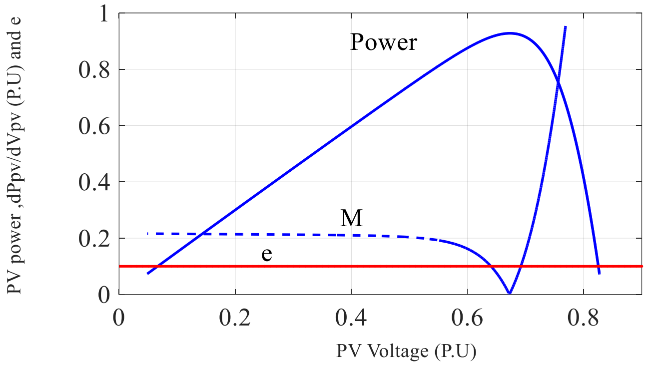

Fig. 3. Basic idea of current IncCon algorithm on P-V curve

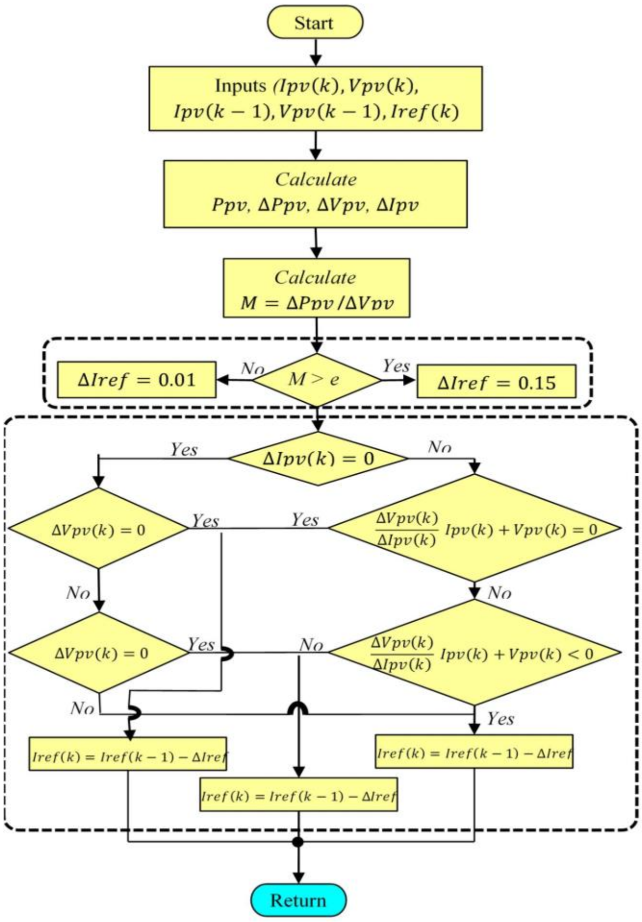

Fig. 4. Flowchart of the proposed MPPT

The proposed MPPT scheme is employed with an algorithm of variable current step size, which is added to the current *IncCon* in order to obtain an enhancement in terms of time response and oscillation around the MPP. A small positive value *e* is considered in order to separate the dynamic and steady states tracking operation. In addition, the calculation of the ratio M is given by equation 6; when *M* is bigger than the chosen positive value *e*, the *ΔIref* takes a big value as well as the MPP will be reached rapidly. Thus, when it is smaller, *ΔIref* will take a small value and consequently, the power oscillation around the MPP will be reduced.

$$M = \left| \frac{dPpv}{dVpv} \right| \tag{6}$$

From Figure 3, it is clear that the ratio *M* takes large values in case where the PV power point is far left and far right from MPP, on the other hand, when PV power is close to MPP, *M* takes very small values. For this reason, the value *e* is chosen small positive value to separate the dynamic and steady states tracking.

Fig.4.represents the flowchart of the proposed current MPPT algorithm.

B. Predictive current control

The role of the predictive controller is to enforce *Ipv* to track *Iref* delivered by the MPPT unit, the determination of the future duty cycle is based on exact knowledge of DC-DC boost converter model (Panagiotis E. Kakosimos et al. , 2013) . Fig.5 illustrates the equivalent circuit of the boost converter considering on and off switching states.

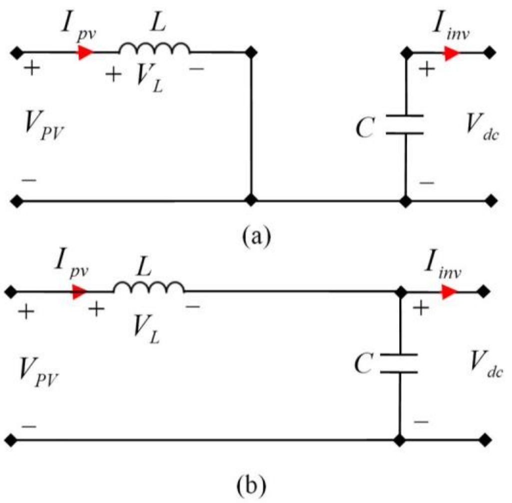

Fig. 5.DC-DC equivalent circuit

When the switch is on, the boost converter equations can be described as follows

$$\begin{cases} L\dfrac{di_{pv}(t)}{dt} = v_{pv}(t) \\ C\dfrac{dv_{dc}(t)}{dt} = -i_{inv}(t) \end{cases} \tag{7}$$

When the switch is off, the boost converter equations yield

$$\begin{cases} L\dfrac{di_{pv}(t)}{dt} = v_{pv}(t) - v_{dc}(t) \\ C\dfrac{dv_{dc}(t)}{dt} = i_{pv}(t) - i_{inv}(t) \end{cases} \tag{8}$$

Equations (7) and (8) can be rewritten in term of duty cycle form as

$$\begin{cases} L\dfrac{di_{pv}(t)}{dt} = v_{pv}(t) - v_{dc}(t) + v_{dc}(t)d(t) \\ C\dfrac{dv_{dc}(t)}{dt} = i_{pv}(t) - i_{inv}(t) - i_{pv}(t)d(t) \end{cases} \tag{9}$$

The discrete time system of Equation (9) considering the sampling frequency is *Ts* as follows (Panagiotis E. Kakosimos et al. , 2013)

$$\begin{cases} i_{pv}(k+1) = i_{pv}(k) + \dfrac{Ts}{L}[v_{pv}(k) + (d(k)-1)v_{dc}(k)] \\ v_{dc}(k+1) = v_{dc}(k) + \dfrac{Ts}{C}[(1-d(k))i_{pv}(k) - i_{inv}(k)] \end{cases} \tag{10}$$

In order to obtain the future duty cycle, Equation (10) can be rewritten as

$$i_{pv}(k+2) = i_{pv}(k+1) + \frac{Ts}{L}[v_{pv}(k+1) + (d(k+1)-1)v_{dc}(k+1)] \tag{11}$$

The current *Ipv* should track the current *Iref* delivered by MPPT unit in three control cycles (Panagiotis E. Kakosimos et al. , 2013)

$$i_{pv}(k+2) = I_{ref}(k) \tag{12}$$

The future tension *Vpv (k+1)* can be estimated as

$$v_{pv}(k+1) \approx v_{pv}(k) \tag{13}$$

From (11), (12) and (13), the future duty cycle can be derived as

$$d(k+1) = \frac{L[I_{ref}(k) - i_{pv}(k+1)] - v_{dc}(k) + v_{pv}(k)}{v_{dc}(k)Ts} \tag{14}$$

1.1 VOC based on predictive control strategy and SVM

In this section, rotating frame *d-q* grid current control is performed through predictive control strategy and space vector modulation. The predictive *Id-q* currents control is based on the calculation of the voltage vector reference which is applied during the next sample time through SVM in order to closes the error between the predicted currents *Id(k+1)*, *Iq(k+1)* and their references *Id_ref*, *Iq_ref*.

Id_ref is estimated by DC-link PI controller, while *Iq_ref* is estimated according to reactive power requested by grid operator

$$i_{q\_ref} = \frac{Q_{ref}}{V_{gd} * 1.5} \tag{15}$$

To apply predictive control strategy, the grid tied inverter model is necessary. The required mathematical model in natural frame *(abc)* is illustrated by (José Rodríguez et al. , 2007):

$$\frac{di_g(t)}{dt} = \frac{1}{L}[V - e_g - Ri_g] \qquad (16)$$

From Equation (16), the grid tied inverter model in rotating frame *d-q* can be expressed in terms of inverter voltages, grid voltages, and filter inductance as follow (Venkata Yaramasu et al., 2014):

$$\begin{cases} \dfrac{di_d(t)}{dt} - wi_q(t) = \dfrac{1}{L}[-Ri_d(t) - e_d(t) + V_d] \\ \dfrac{di_q(t)}{dt} + wi_d(t) = \dfrac{1}{L}[-Ri_q(t) - e_q(t) + V_q] \end{cases} \qquad (17)$$

Euler forward method is used to approximate the derivatives in the Equations (17) in order to obtain discrete time model given below

$$\begin{cases} \dfrac{di_d(t)}{dt} = \dfrac{i_d(k+1) - i_d(k)}{T_s} \\ \dfrac{di_q(t)}{dt} = \dfrac{i_q(k+1) - i_q(k)}{T_s} \end{cases} \qquad (18)$$

where *Ts* is the sampling time.

The discrete time model of Equation (17) yields:

$$\begin{cases} i_d(k+1) = \dfrac{T_s}{L}[-Ri_d(k) - e_d(k) + V_d(k)] + T_s wi_q(k) - i_d(k) \\ i_q(k+1) = \dfrac{T_s}{L}[-Ri_q(k) - e_q(k) + V_q(k)] - T_s wi_d(k) - i_q(k) \end{cases} \qquad (19)$$

To calculate the voltage vector reference, the synchronous frame currents *Id-Iq* should track their references *Id_ref-Iq_ref* during the next sampling time which means (Panagiotis E. Kakosimos et al. , 2013):

$$\begin{cases} i_d(k+1) = i_{d\_ref} \\ i_q(k+1) = i_{q\_ref} \end{cases} \qquad (20)$$

Where:

$$\begin{cases} i_d(k) = i_{d\_mes} \\ i_q(k) = i_{q\_mes} \end{cases} \qquad (21)$$

$$\begin{cases} e_d(k) = e_{d\_mes} \\ e_q(k) = e_{q\_mes} \end{cases} \qquad (22)$$

By substituting equations (20) (21) (22) in (19), the voltage vector reference can be given as:

$$\begin{cases} V_d = \dfrac{L}{Ts}(i_{d\_ref} - i_{d\_mes}) + Ri_{d\_mes} + e_{d\_mes} - wLi_{q\_mes} \\ V_q = \dfrac{L}{Ts}(i_{q\_ref} - i_{q\_mes}) + Ri_{q\_mes} + e_{q\_mes} + wLi_{d\_mes} \end{cases} \qquad (23)$$

The reference voltage vector *Vd*, *Vq* is applied during the next sampling time through space vector modulation (SVM)

Table 1. Global system parameters

PV Siemens SM110 electrical parameters	**Value**
Maximum power (Pmpp)	110*Watts*
Open circuit voltage (Voc)	43.5*V*
Short circuit current (Isc)	3.45*A*
Voltage at Pmax	*35*
current at Pmax	*3.15*
Number of cells connected in parallel (Np)	1
Number of cells connected in series (Ns)	72
Number of modules connected in series (Nss)	2
Number of modules connected in parallel (Npp)	2
Boost converter electrical parameters	**Value**
Resistor R	50Ω
Inductor L	40 *mH*
Capacitor C	1100μF
Grid electrical parameters	**Value**
Grid inductance *Lg*	10 mH
Grid resistance *Rg*	0.1 Ω
Grid Voltage *Vg*	50 V
Grid frequency *Fg*	50 Hz
Simulation Parameters	**Value**
MPPT sampling Time *Ts*	0.001s
SVM frequency Fm	30 Khz
PWM frequency Fp	30 Khz

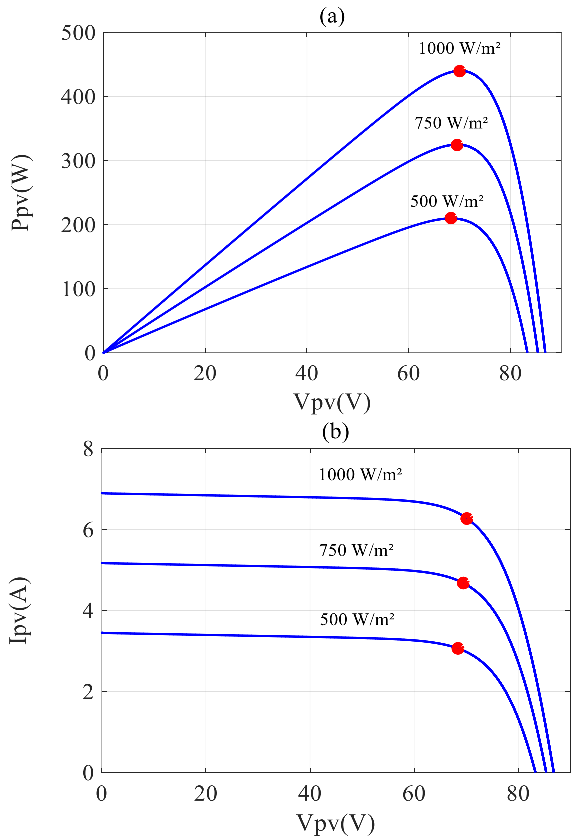

Fig. 6. PV system characteristics: (a) P (V); (b) I (V).

4. RESULTS AND DISCUSION

Extensive simulations with the parameters shown in Table 1 are performed in the global system using MAT LAB/Simulink and Simpower system packages in order to evaluate the proposed control scheme performance. Figure 6 shows the PV array characteristics P-V I-V used in the simulation.

This study is divided into two parts. In the first one, the purpose is to compare the proposed MPPT (V-S IncCon/PPC) performance with (IncCon/PCC) and conventional IncCon in terms of MPP tracking speed, accuracy and oscillations. The second part, VOC based on predictive control strategy and space vector modulation (PS-VOC) is applied to control the second stage in order to inject the extracted PV power with high grid current quality under irradiation changes and reactive power requested by grid operator.

4.1 VS-INC/PCC versus INC/PCC comparaison

Under irradiation changes represented in Figure 7 (b), the proposed MPPT method, IncCon algorithm based on PCC and conventional IncCon are tested by numerical simulation. Initially, the irradiance level is set to 500 W/m^2. Then, at 0.1 s, a sudden increase irradiation change from 500 to 700 W/m^2 is occurred. The proposed method reaches the MPP during 0.007 s, the IncCon/PCC takes 0.018 s. While the conventional method reach the MPP during 0.034 s with drift of the tracking direction. Then the irradiation level is decreased slowly from 800 to 400 W/m^2 during 0.2 s. The proposed method exhibits better accuracy tracking than both INC/PCC and conventional IncCon as shown in Figure 8. Finally, a sudden irradiation from 400 to 1000 W/m^2 occurs at 0.5 s, the improved MPPT shows also a faster tracking than both IncCon/PCC and conventional MPPT, where the proposed MPPT takes just 0.025 s to reach the MPP while the IncCon/PCC needs 0.056 s and conventional MPPT needs 0.1s as shown in Figure 7 (a).

In another side, the proposed MPPT shows a high performance in term of power oscillation compared to IncCon/PCC and conventional one as depicted in Figure 8, where the oscillation widths around MPPs, by using the proposed method, under different steady irradiations levels (500, 700,400 and 1000 watts/m²) are, [209.7 209.2], [302 301.6], [163.8, 163.4], [440 439.8] respectively. In counterpart, the widths of power oscillation by using the IncCon/PCC method are [209.7 208.5], [302,300.5], [163.8, 162.2], [440,439.4] respectively, and when using the conventional one are [209.7 206], [302,299], [163.8, 161], [440,437.2] respectively.

IncCon through predictive current control strategy responds to the change in irradiation rapidly and accuracy than the conventional algorithm as shown by the simulation results, due to the linear relationship between the irradiance and the PV current. While, the developed variable step size current Incremental conductance algorithm provides the proposed MPPT more valuable than the IncCon/PCC in terms of speed tracking and oscillations. It generates high *ΔIref* during a sudden irradiations and a small *ΔIref* for fixed or slow irradiation changes. Furthermore, the conventional INC generates a fixed *ΔIref* under all irradiation changes as shown in Figure 9.

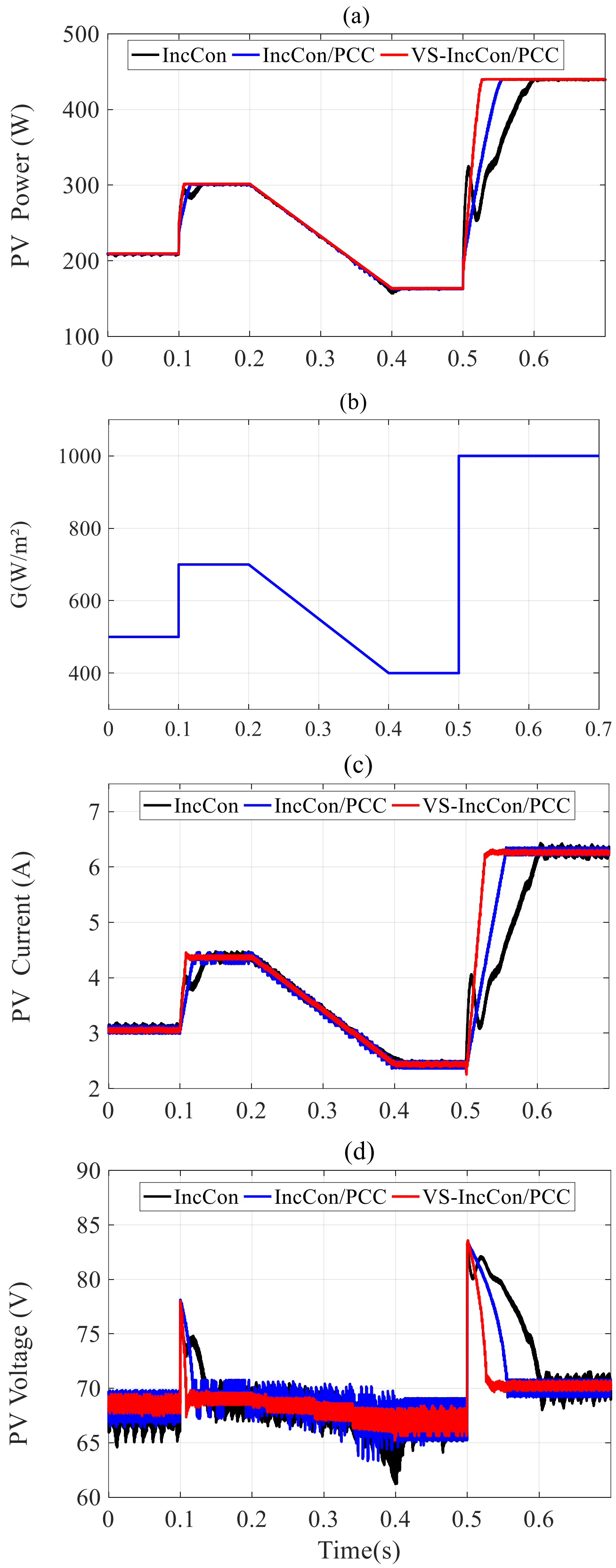

Fig.7. Performance of IncCon, IncCon/PCC, Proposed MPPT under irradiation changes

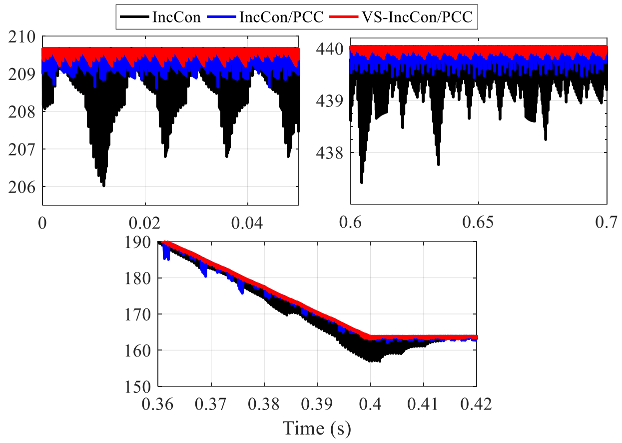

Fig. 8 Zoom of PV power output

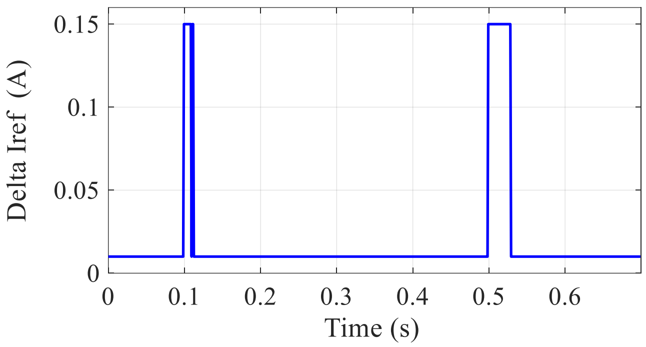

Fig. 9. Behaviour of proposed VS-IncCon

4.2 Performance of PS-VOC under irradiation changes

This section deals with test of the global system performance under different irradiation changes and presents the efficiency of the applied method in terms of *d_q* currents control and grid current THD.

Firstly, as illustrated in Figure 10.a, for a fixed irradiation condition at 500 W/m² during the interval [0, 0.1s [, the PV array output is oscillating around the MPP and the *Vdc* is completely maintained to its reference. Hence, *Id* and *Iq* are regulated according to their references by virtue of the proposed method (PS-VOC), as observed in Figure 10.c, d. Furthermore, the grid currents are balanced and sinusoidal.

Afterward, the sudden irradiation change from 500 to 700 W/m² at instant 0.1s leads to an increase in the PV power output and a small deviation in *Vdc* over its reference as shown in Figure 10.a, b. Despite that, *Id* and *Iq* remain tracking their references, whereas the grid currents are increased and kept sinusoidal due to the capability of the proposed method.

Then, under the slow irradiation change from 700 to 400 W/m² during 0.2 to 0.4s, the PV power slowly decreases. Also, *Vdc* is a bit far from its reference as illustrated in Figure 10.b. Meanwhile, *Id_Iq* currents track their references and grid currents are decreasing with a sinusoidal form.

Finally, a large sudden change in irradiation occurs at instant 0.5 s. The PV power output is rapidly increased, which leads to a large deviation of *Vdc* from its reference, as shown

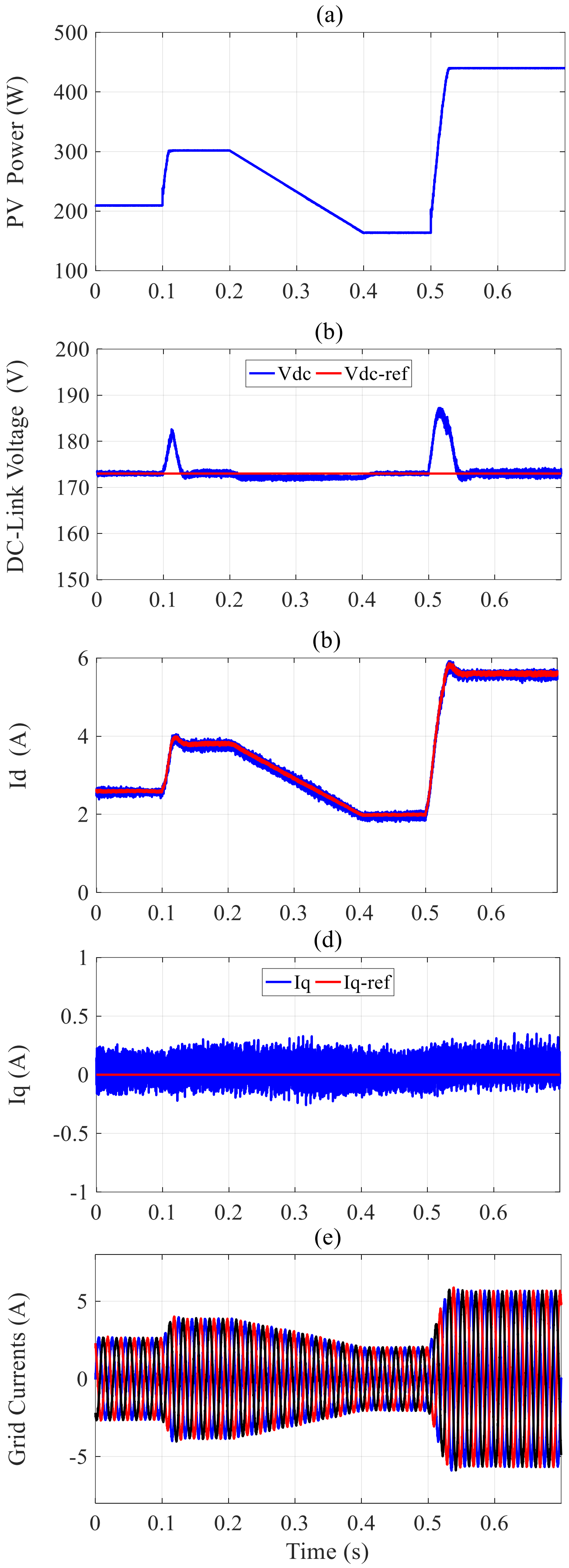

Fig. 10. Performance of global system under irradiation changes.

in Figure 10.b. Even though, *Id* and *Iq* remain tracking their references whereas the grid currents remain sinusoidal form. This due to efficiency of the proposed method.

As presented in Table 2, the proposed method (VOC based on predictive strategy through SVM) provides high grid current quality under all irradiation change level cases according to the international standards (IEEE-519, THD < 5%).

Table.2 Obtained THD under different irradiation levels

	500 W/m²	700 W/m²	Increase 700-400 W/m²	400 W/m²	1000 W/m²
THD%	3.56	2.66	2.99	4.08	1.51

4.3 Performance of PS-VOC under reactive power reference changes

In this section, the performance of the proposed PS-VOC is examined under reactive power reference changes and fixed PV power output at 440 W.

As shown in Figure 11, the reactive power reference is set to zero during [0 0.2s [, hence, the *Iq_ref* is also set to zero. The DC-link voltage is completely maintained to its reference, when the *Id-Iq* currents track their references and the grid currents are sinusoidal.

Next, at instant 0.2 s, a sudden increase from 0 to 300 VAR is occurred in the reactive power reference while, the *Iq* reference is estimated to be 4 A. The proposed PS-VOC method shows a rapid *Iq* tracking to its reference (0.0027s). Besides, the grid currents increase rapidly due to the increase in grid apparent power *Sg* where the grid current amplitude is proportional to *Sg*. It is observed also that, the angle between the grid currents and grid voltages is changed as depicted in Figure 12.a.

Then, at instant 0.4 s, a sudden decrease from 300 to 0 VAR in the reactive power reference is occurs while, *Iq_ref* is set to 0A. The ability of the proposed PS-VOC shows a rapid tracking of *Iq* to its reference (0.004s). Also, the grid currents amplitude increase due the increase of apparent power *Sg*. While the grid currents and voltages are comeback in phase as illustrated in Figure 12.b.

Finally, at instant 0.6 s another sudden decrease from 0 to -300 is occurs again in the reactive power reference while *Iq_ref* is estimated to be -4 A. The proposed VOC method enforces *Iq* to reach its reference in only 0.0037s. Also, the grid currents are rapidly increased due to the increase in grid apparent power *Sg*. Where, the grid current amplitude is proportional to *Sg*. the phase between the grid currents and voltages is changed as depicted in Figure 12.c.

The proposed method (VOC based on predictive strategy trough SVM) provides high grid current quality under all reactive power reference change levels according to the international standards (IEEE-519, THD < 5%), as presented in Table 3.

Table. 3 Obtained THD under different reactive power reference levels

	0 VAR	300 VAR	-300 VAR
THD%	1.51	1.45	1.30

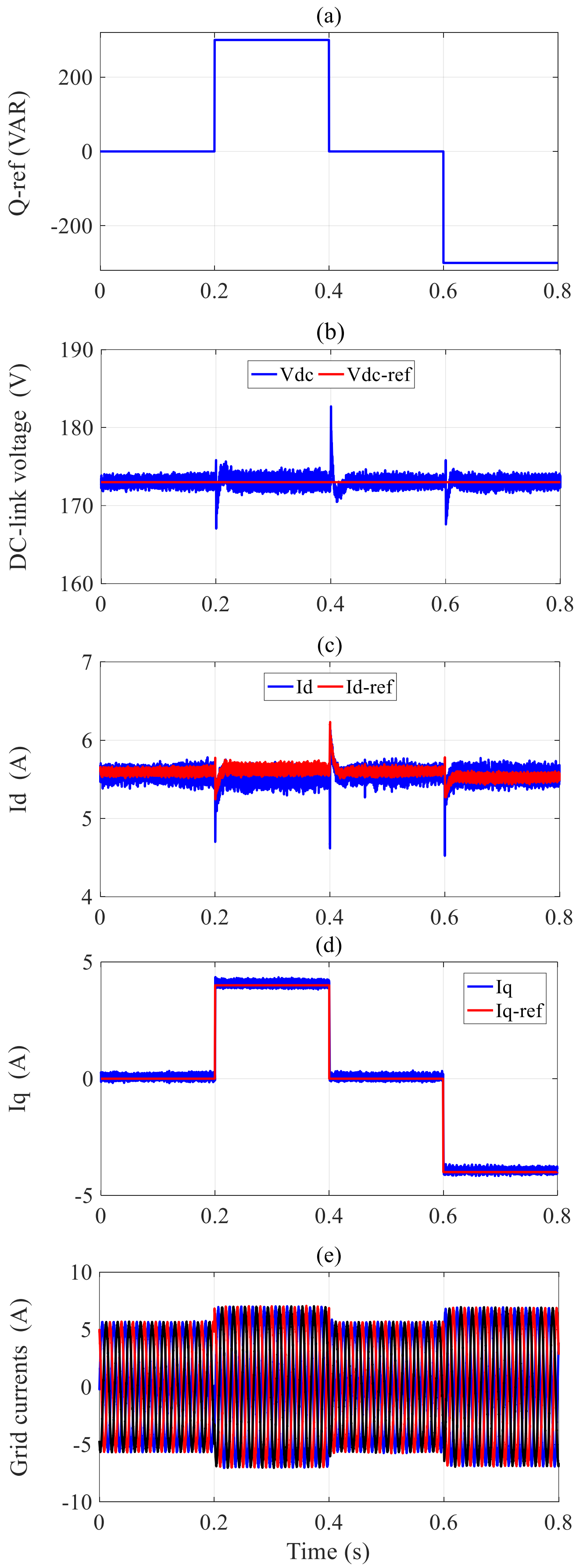

Fig. 11.Performance of global system under reactive power grid operator request changes.

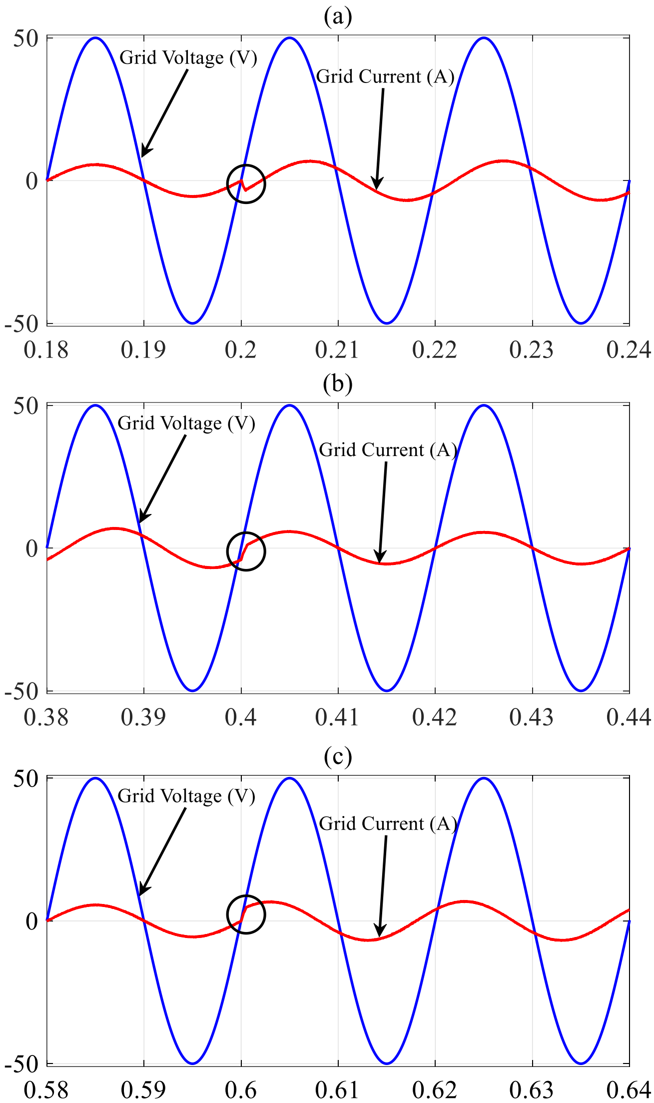

Fig. 12 Grid current and voltage phase change under reactive power change.

5. CONCLUSIONS

In this paper, an improved control scheme based on predictive control strategy for three phase dual-stage grid connected photovoltaic (PV) system is presented. Variable step size current Incremental conductance through predictive current control (VS-IncCon/PCC) is proposed and applied to the first stage in order to track the maximum power point rapidly and accurately. Whereas the VOC based on predictive control strategy through SVM (PS-VOC) is employed to control the second stage in order to inject the extracted PV power as well as reactive power of grid operator request with high grid currents quality. The simulation results show a significant enhancement by applying the proposed MPPT method in comparison with the conventional IncCon and IncCon through PCC methods in terms of accuracy tracking, response time and stability around the maximum power point under irradiation changes. Moreover, the proposed control of grid tied two-level inverter (PS-VOC) presents high grid current quality in accordance with international standards (IEEE-519) for any irradiation and reactive power changes.

6. REFERENCES

Abdelghani Harrag, Sabir Messalti, (2015). Variable step size modified P&O MPPT algorithm using GA-based hybrid offline/online PID controller, Renewable and Sustainable Energy Reviews, Vol. 49, pp. 1247-1260.

Abdelhamid Loukriz, Mourad Haddadi and Sabir Messalti, (2016).Simulation and experimental design of a new advanced variable step size Incremental Conductance MPPT algorithm for PV systems, ISA transactions, Vol. 62, pp. 30-38.

Abdelkrim Menadi, Sabrina Abdeddaim , Ahmed Ghamri and Achour Betka,(2015). Implementation of fuzzy-sliding mode based control of a grid connected photovoltaic system, ISA transactions, Vol. 58, pp. 586-594.

Antoneta Iuliana Bratcu, Iulian Munteanu, Seddik Bacha, Bertrand Raison, (2008). Maximum Power Point Tracking of Grid-connected Photovoltaic Arrays by Using Extremum Seeking Control, Journal of Control Engineering and Applied Informatics, Vol. 10, pp. 3-12.

Azadeh Safari and Saad Mekhilef, (2011). Simulation and Hardware Implementation of Incremental Conductance MPPT With Direct Control Method Using Cuk Converter, IEEE Transactions on Industrial Electronics, Vol. 58, pp. 1154-1161.

Azzouzi M., (2013). Optimization of Photovoltaic Generator by Using P&O Algorithm Under Different Weather Conditions, Journal of Control Engineering and Applied Informatics, Vol. 15, pp. 12-19.

Boualem Bendib, Hocine Belmili and Fateh Krim (2015). A survey of the most used MPPT methods: Conventional and advanced algorithms applied for photovoltaic systems, Renewable and Sustainable Energy Reviews, Vol. 45, pp. 637-648.

Chinmay Jain and Bhim Singh, (2017). A Three-Phase Grid Tied SPV System with Adaptive DC Link Voltage for CPI Voltage Variations, IEEE Transactions on Sustainable Energy, Vol. 7, pp. 337-344.

Enrico Bianconi, Javier Calvente, Roberto Giral, Emilio Mamarelis, Giovanni Petrone, Carlos Andrés Ramos-Paja, Giovanni Spagnuolo and Massimo Vitelli, (2013). A fast current-based MPPT technique employing sliding mode control, IEEE Transactions on Industrial Electronics, Vol. 60, pp. 1168-1178.

Fangrui Liu, Shanxu Duan, Fei Liu, Bangyin Liu, and Yong Kang, (2008). A Variable Step Size INC MPPT Method for PV Systems, IEEE Transactions on Industrial Electronics, Vol. 55, pp. 2622-2628.

Fernando M. de Oliveira, Sérgio A. Oliveira da Silva, Fábio R. Durand and Leonardo P. Sampaio, (2016). Grid-tied photovoltaic system based on PSO MPPT technique with active power line conditioning, IET Power Electronics, Vol. 9,pp.1180-1191.

Houria Boumaaraf, Abdelaziz Talha and Omar Bouhali,(2015).A three-phase NPC grid-connected inverter for photovoltaic applications using neural network MPPT, Renewable and Sustainable Energy Reviews, Vol. 49, pp. 1171-1179.

Jiabing Hu and Z. Q. Zhu, (2011). Investigation on Switching Patterns of Direct Power Control Strategies for Grid-Connected DC–AC Converters Based on Power Variation

Rates, IEEE Transactions on Power Electronics, Vol. 26, pp. 3582-3598.

José Rodríguez, Jorge Pontt, César A. Silva, Pablo Correa, Pablo Lezana, Patricio Cortés, and Ulrich Ammann (2007). Predictive current control of a voltage source inverter, IEEE Transactions on Industrial Electronics, Vol. 54, pp. 495-503.

Lin Chen, Ahmadreza Amirahmadi, Qian Zhang, Nasser Kutkut and Issa Batarseh,(2014). Design and implementation of three-phase two-stage grid-connected module integrated converter, IEEE Transactions on Power Electronics,Vol 29, pp. 3881-3892.

Mahrous El-Sayed Ahmed, Mohamed Orabi, Omar Mohamed AbdelRahim, (2013). Two-stage micro-grid inverter with high-voltage gain for photovoltaic applications, IET Power Electronics, Vol. 6, pp. 1812-1821.

Mariusz Malinowski, Marek Jasin´ski and Marian P. Kazmierkowski, (2004). Simple Direct Power Control of Three-Phase PWM Rectifier Using Space-Vector Modulation (DPC-SVM) IEEE Transactions on Industrial Electronics, Vol. 51, pp. 447-454.

Mariusz Malinowski, Marian P. Kazmierkowski, Steffan Hansen, Frede Blaabjerg and G. D. Marques,M, (2001). Virtual Flux Based Direct Power Control of Three-phase PWM Rectifiers, IEEE Transactions on industry applications, Vol. 37, pp.1019-1027.

Mohamed M. Algazar, Hamdy AL-monier, Hamdy Abd EL-halim and Mohamed Ezzat El Kotb Salem, (2012). Maximum power point tracking using fuzzy logic control, Electrical Power and Energy Systems, Vol. 39, pp. 21–28.

Muhammad Ammirrul Atiqi Mohd Zainuri, Mohd Amran Mohd Radzi, Azura Che Soh and Nasrudin Abd Rahim, (2013). Development of adaptive perturb and observe-fuzzy control maximum power point tracking for photovoltaic boost dc–dc converter, IET Renewable Power Generation, Vol. 8, pp. 183–194.

Panagiotis E. Kakosimos, Antonios G. Kladas, (2011). Implementation of photovoltaic array MPPT through fixed step predictive control technique, Renewable Energy, Vol. 36, pp. 2508-2514.

Panagiotis E. Kakosimos, Antonios G. Kladas and Stefanos N. Manias, (2013). Fast photovoltaic-system voltage-or current-oriented MPPT employing a predictive digital current-controlled converter, IEEE Transactions on Industrial Electronics, Vol. 60, pp. 5673-5685.

Raseswari Pradhan and Bidyadhar Subudhi, (2016). Double Integral Sliding Mode MPPT Control of a Photovoltaic System, IEEE Transactions on Control Systems Technology, Vol. 24, pp. 285-292.

Rong-Jong Wai, Wen-Hung Wang, and Chung-You Lin, (2008). High-Performance Stand-Alone Photovoltaic Generation System, *IEEE Transactions on Industrial Electronics*, Vol. 55, pp. 240–250.

Sathish Kumar Kollimalla and Mahesh Kumar Mishra, (2014). A Novel Adaptive P&O MPPT Algorithm Considering Sudden Changes in the Irradiance, IEEE Transactions on Energy Conversion, vol. 29, pp. 602-610.

Tawfik Radjai, Lazhar Rahmani, Saad Mekhilef and Jean Paul Gaubert, (2014). Implementation of a modified incremental conductance MPPT algorithm with direct control based on a fuzzy duty cycle change estimator using dSPACE, Solar Energy, Vol.110, pp. 325–337.

Teodorescu Remus, Liserre Marco and Rodriguez Pedro, (2011). Grid converters for photovoltaic and wind power systems. John Wiley & Sons.

Venkata Yaramasu, Bin Wu and Jin Chen (2014). Model-Predictive Control of Grid-Tied Four-Level Diode-Clamped Inverters for High-Power Wind Energy Conversion Systems, IEEE Transactions on Power Electronics, Vol. 29,pp.2861-2873.